Theory of aberration fields for general optical systems with freeform surfaces

Kyle Fuerschbach,[1,*] Jannick P. Rolland,[1] and Kevin P. Thompson[1,2]

[1]*The Institute of Optics, University of Rochester, 275 Hutchinson Road, Rochester, New York 14627, USA*
[2]*Synopsys Inc., 3 Graywood Lane, Pittsford, New York 14534, USA*
[*]*fuerschb@optics.rochester.edu*

Abstract: This paper utilizes the framework of nodal aberration theory to describe the aberration field behavior that emerges in optical systems with freeform optical surfaces, particularly φ-polynomial surfaces, including Zernike polynomial surfaces, that lie anywhere in the optical system. If the freeform surface is located at the stop or pupil, the net aberration contribution of the freeform surface is field constant. As the freeform optical surface is displaced longitudinally away from the stop or pupil of the optical system, the net aberration contribution becomes field dependent. It is demonstrated that there are no new aberration types when describing the aberration fields that arise with the introduction of freeform optical surfaces. Significantly it is shown that the aberration fields that emerge with the inclusion of freeform surfaces in an optical system are exactly those that have been described by nodal aberration theory for tilted and decentered optical systems. The key contribution here lies in establishing the field dependence and nodal behavior of each freeform term that is essential knowledge for effective application to optical system design. With this development, the nodes that are distributed throughout the field of view for each aberration type can be anticipated and targeted during optimization for the correction or control of the aberrations in an optical system with freeform surfaces. This work does not place any symmetry constraints on the optical system, which could be packaged in a fully three dimensional geometry, without fold mirrors.

OCIS codes: (080.1010) Aberrations (global); (080.4228) Nonspherical mirror surfaces.

References and links

1. K. Fuerschbach, G. E. Davis, K. P. Thompson, and J. P. Rolland, "Assembly of a freeform off-axis optical system employing three φ-polynomial Zernike mirrors," Opt. Lett. **39**(10), 2896–2899 (2014).
2. K. Fuerschbach, J. P. Rolland, and K. P. Thompson, "A new family of optical systems employing φ-polynomial surfaces," Opt. Express **19**(22), 21919–21928 (2011).
3. R. V. Shack and K. P. Thompson, "Influence of alignment errors of a telescope system," Proc. SPIE **251**, 146–153 (1980).
4. K. Thompson, "Description of the third-order optical aberrations of near-circular pupil optical systems without symmetry," J. Opt. Soc. Am. A **22**(7), 1389–1401 (2005).
5. K. P. Thompson, "Aberration fields in unobscured mirror systems," J. Opt. Soc. Am. **103**, 159–165 (1980).
6. T. Schmid, J. P. Rolland, A. Rakich, and K. P. Thompson, "Separation of the effects of astigmatic figure error from misalignments using nodal aberration theory (NAT)," Opt. Express **18**(16), 17433–17447 (2010).
7. K. Fuerschbach, J. P. Rolland, and K. P. Thompson, "Extending nodal aberration theory to include mount-induced aberrations with application to freeform surfaces," Opt. Express **20**(18), 20139–20155 (2012).
8. K. Fuerschbach, J. P. Rolland, and K. P. Rolland-Thompson, "Nodal aberration theory applied to freeform surfaces," in *Classical Optics 2014* (Optical Society of America, 2014), ITh2A.5.
9. K. Fuerschbach, "Freeform, phi-polynomial optical surfaces: optical design, fabrication and assembly," Ph.D. (The University of Rochester, 2014).
10. R. W. Gray, C. Dunn, K. P. Thompson, and J. P. Rolland, "An analytic expression for the field dependence of Zernike polynomials in rotationally symmetric optical systems," Opt. Express **20**(15), 16436–16449 (2012).

#217287 - $15.00 USD Received 18 Jul 2014; revised 12 Sep 2014; accepted 22 Sep 2014; published 20 Oct 2014

11. J. Wang, B. Guo, Q. Sun, and Z. Lu, "Third-order aberration fields of pupil decentered optical systems," Opt. Express **20**(11), 11652–11658 (2012).
12. C. R. Burch, "On the optical see-saw diagram," Mon. Not. R. Astron. Soc. **102**(3), 159–165 (1942).
13. A. Rakich, "Calculation of third-order misalignment aberrations with the optical plate diagram," Proc. SPIE **7652**, 765230 (2010).
14. K. P. Thompson, T. Schmid, O. Cakmakci, and J. P. Rolland, "Real-ray-based method for locating individual surface aberration field centers in imaging optical systems without rotational symmetry," J. Opt. Soc. Am. A **26**(6), 1503–1517 (2009).
15. J. C. Wyant and K. Creath, "Basic wavefront aberration theory for optical metrology," in *Applied Optics and Optical Engineering*, R. R. Shannon and J. C. Wyant, eds. (Academic, 1992), pp. 1–53.
16. K. P. Thompson, T. Schmid, and J. P. Rolland, "The misalignment induced aberrations of TMA telescopes," Opt. Express **16**(25), 20345–20353 (2008).
17. K. P. Thompson, "Multinodal fifth-order optical aberrations of optical systems without rotational symmetry: the comatic aberrations," J. Opt. Soc. Am. A **27**(6), 1490–1504 (2010).
18. K. P. Thompson, "Multinodal fifth-order optical aberrations of optical systems without rotational symmetry: the astigmatic aberrations," J. Opt. Soc. Am. A **28**(5), 821–836 (2011).
19. J. E. Stacy and S. A. Macenka, "Optimization of an unobscured optical system using vector aberration theory," Proc. SPIE **679**, 21–24 (1986).
20. K. P. Thompson, "Multinodal fifth-order optical aberrations of optical systems without rotational symmetry: spherical aberration," J. Opt. Soc. Am. A **26**(5), 1090–1100 (2009).
21. K. P. Thompson, "Aberration fields in tilted and decentered optical systems," Ph.D. (The University of Arizona, 1980).
22. C. Menke, "What's in the Designer's Toolbox for Freeform Systems?" in *Renewable Energy and the Environment* (Optical Society of America, 2013), FM4B.1.

1. Introduction

Freeform optical surfaces present new possibilities for the efficient packaging of an optical system and, with current fabrication technologies, can be manufactured and assembled to create high performing optical systems as recently demonstrated [1]. While design strategies exist to aid the optical designer in the effective optimization of systems with freeform surfaces, the approaches are predominately empirical [2] and are in need of an analytical theory to support the proposed techniques. Since the freeform surfaces are inherently nonsymmetric, their aberration behavior requires a theory that assumes no symmetry in the optical system.

One foundation that describes the aberration behavior of optical systems that lack symmetry is nodal aberration theory (NAT). The theory, discovered by Shack [3] and developed by Thompson [4], describes the behavior of an optical system with rotationally symmetric components, or offset aperture portions thereof, that may be tilted and/or decentered [5]. The addition of a nonsymmetric optical component into NAT was first developed by Schmid et al. [6] where NAT was used to describe the aberration behavior of an astigmatic optical surface located at the aperture stop (or pupil). At this specific location of the optical system, the beam footprint for all field points is the same and fills the entire optical surface. In this case, the net aberration contribution of the astigmatic surface is field constant. Recently, Fuerschbach et al. [7] implemented a generalized approach where the nonsymmetric optical surface could lie anywhere in the optical system. In this case, importantly, the net aberration contribution is field dependent. Many aberration components may contribute to this field dependent behavior, each having a unique orientation and magnitude throughout the field that scales with the distance of the freeform surface relative to the stop or pupil. Specifically, Fuerschbach analyzed the behavior of three point mount error that induces a deformation on an optical surface that relates closely to Zernike trefoil. When an optical surface is deformed by a mounting error on a surface away from the stop, there is a field dependent astigmatic contribution known as field conjugate, field linear astigmatism in addition to the anticipated field constant elliptical coma contribution [7].

In this paper, the approach set forth by Fuerschbach [7–9] is described for the emerging class of freeform optical surfaces known as φ-polynomial surfaces. The sag of these surfaces varies not only with the radial component, ρ, but also with the azimuthal component, φ. The specific type of φ-polynomial surface to be explored in this work is the Fringe Zernike

#217287 - $15.00 USD Received 18 Jul 2014; revised 12 Sep 2014; accepted 22 Sep 2014; published 20 Oct 2014

polynomial set up to sixth order [10]. In this paper it is demonstrated that including φ-polynomial freeform surfaces into NAT does not introduce aberrations with new forms of field dependence; rather, the freeform parameters link to the terms presented for the generally multinodal field dependence of the fourth and sixth order wavefront aberrations derived for tilted and/or decentered rotationally symmetric surfaces. While these terms have existed in NAT, some higher order terms have not been observed in the case of tilted and decentered systems following a small misalignment because their magnitude was typically negligible relative to the dominant lower order misalignment induced components. In the case of optical systems designed with freeform surfaces that have large tilts and decenters, these unique field dependences, to be presented, tend to dominate. It was part of design process of an optical system with freeform surfaces that these forms were discovered and the first discovery reported in [7] led us to further revisit NAT to fully develop the aberration field behavior of freeform surfaces.

2. Theoretical formulation of the field dependent aberration behavior of freeform, φ-polynomial surfaces away from the aperture stop

In order to characterize the impact of a freeform, φ-polynomial optical surface away from the stop on the net aberration field, consider first a classical Schmidt telescope configuration with a small enough magnitude field of view (FOV) so that only third order aberrations are of concern and the higher order aberrations are negligible. The telescope is composed of a rotationally symmetric third order (fourth order in wavefront) aspheric corrector plate coincident with a mechanical aperture that is the stop of the optical system, located at the center of curvature of a spherical mirror. By locating the stop at the center of curvature of the spherical mirror, third order coma and astigmatism are corrected. Also with the aspheric corrector plate at the stop surface, the beam footprint on the corrector plate is the same for all field points so the plate only contributes third order spherical aberration that cancels the spherical aberration contribution of the spherical mirror. In this configuration, the system is now corrected for coma, astigmatism, and spherical aberration so only field curvature is left as the limiting third order aberration.

If the aspheric corrector plate is shifted longitudinally along the optical axis relative to the physical aperture stop, as shown in Fig. 1(a), the beam for an off-axis field point will displace across the plate; thus, each field point receives a different contribution from the surface. This beam displacement results in a total surface aberration contribution that encompasses all the field dependent third order aberrations in addition to third order spherical aberration.

To describe this field dependent aberration generation, the amount of relative beam displacement, $\Delta\vec{h}$, must be defined and is given by

$$\Delta\vec{h} \equiv \left(\frac{\bar{y}}{y}\right)\vec{H} = \left(\frac{\bar{u}t}{y}\right)\vec{H}, \tag{1}$$

where $\bar{y}$ is the paraxial chief ray height on the aspheric plate, y is the paraxial marginal ray height on the aspheric plate, $\bar{u}$ is the paraxial chief ray angle, t is the distance between the aspheric corrector plate and the mechanical aperture that is the aperture stop, and $\vec{H}$ is the normalized two-dimensional field vector that locates the field point of interest in the image plane (i.e. $0 \le |\vec{H}| \le 1$). Conceptually, the beam displacement on the aspheric corrector plate when it is located away from the stop can be thought of as a field dependent decenter of the corrector plate when it is located at the stop as depicted in Fig. 1(b). The case where an aspheric corrector plate located at the stop or pupil of an optical system is decentered from the optical axis was previously investigated using NAT by Thompson [5] and was recently revisited by Wang et al. [11]. Taking a similar approach, the net aberration contribution of the aspheric corrector plate, $W(\vec{\rho})$, that only depends on the normalized pupil vector, $\vec{\rho}$, and

#217287 - $15.00 USD Received 18 Jul 2014; revised 12 Sep 2014; accepted 22 Sep 2014; published 20 Oct 2014

not the field vector since the surface is located at the stop, must be remapped to a modified pupil vector, $\vec{\rho}'$. This modified pupil vector relates the beam displacement to the original pupil vector, that is,

$$W(\vec{\rho}) \Rightarrow W\left(\vec{\rho}' + \Delta\vec{h}\right), \tag{2}$$

where it may be recognized that the final measurement is done in the shifted pupil coordinate and the primes can be dropped from the final expression of the net aberration contribution to simplify the notation moving forward. Since $\Delta\vec{h}$ is proportional to $\vec{H}$, the modified net aberration contribution becomes field dependent when the plate is shifted away from the stop surface. For the aspheric corrector plate that generates third order spherical aberration at the stop surface, third order coma, field curvature, astigmatism, distortion, and piston are generated as the corrector plate is axially displaced from the stop surface [7, 12, 13]. The generation of these field dependent aberration terms is not restricted to rotationally symmetric corrector plates and can be applied to the class of freeform, φ-polynomial surfaces. To apply this approach to φ-polynomial surfaces requires relating the φ-polynomial surface to the field constant aberration it induces at the stop surface and then applying the perturbation described in Eq. (2) to establish what field dependent aberration components are induced when the φ-polynomial surface is displaced longitudinally from the stop surface.

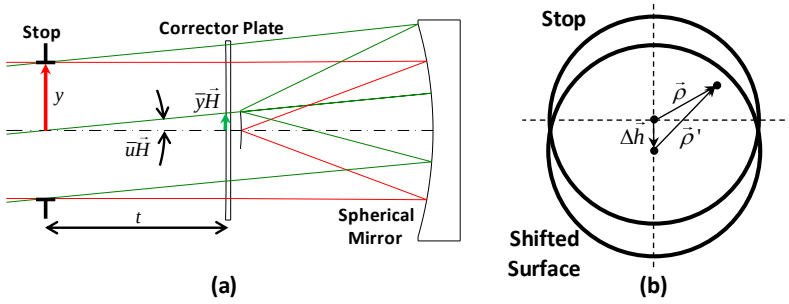

Fig. 1. (a) When the aspheric corrector plate of a Schmidt telescope is displaced longitudinally from the aperture stop along the optical axis, the beam for an off-axis field point will displace across the corrector plate. The amount of relative beam displacement defined by Eq. (1) depends on the paraxial quantities for the marginal ray height, y, the chief ray height, $\bar{y}$, the chief ray angle, $\bar{u}$, and the distance between the stop and the corrector plate, t. (b) The beam displacement on the corrector plate, $\Delta\vec{h}$, can be thought of as a field dependent decenter of the aspheric corrector at the stop that modifies the mapping of the normalized pupil coordinate from $\vec{\rho}$ to $\vec{\rho}'$.

3. The aberration fields of freeform, φ-polynomial surface overlays

The set of φ-polynomial overlays to be placed on an optical surface is the Fringe Zernike polynomial set that is presented in Fig. 2 through sixth order. This set differs from other Zernike polynomial sets in its arrangement of terms where they are ordered by wavefront expansion order, with the fourth order aberration components appearing before the sixth order components. Out of the sixteen terms displayed in Fig. 2, twelve are nonsymmetric, φ-polynomial types and of the twelve nonsymmetric terms, ten will blur the image if they are placed on a surface of an optical system. Moreover, these ten terms form five pairs to be explored, namely, they are Zernike astigmatism ($Z_{5/6}$), Zernike coma ($Z_{7/8}$), Zernike elliptical coma or trefoil ($Z_{10/11}$), Zernike oblique spherical aberration or secondary astigmatism ($Z_{12/13}$), and Zernike fifth order aperture coma or secondary coma ($Z_{14/15}$). The rotationally symmetric terms, defocus (Z_4), Zernike spherical aberration (Z_9), and Zernike fifth order spherical

#217287 - $15.00 USD Received 18 Jul 2014; revised 12 Sep 2014; accepted 22 Sep 2014; published 20 Oct 2014

aberration (Z_{16}), need not be addressed since they are currently handled by the aspheric sigma vector in NAT [14].

In Section 2, when describing the aspheric corrector plate of the Schmidt telescope, it was found that the aberration contribution from the corrector plate is field constant when the plate is located at the aperture stop and develops a field dependent contribution as the plate is shifted longitudinally away from the aperture stop. For the aspheric corrector plate of the Schmidt telescope, the resulting field constant aberration is third order spherical aberration. By analogy, if a plate at the stop is deformed by one of the Zernike terms described above, it will also introduce a field constant aberration. By utilizing the vector pupil dependence of the Zernike overlay terms, the induced field constant aberration, predicted by NAT, can be added to the total aberration field. From this initial field constant aberration, the field dependent nature can then be developed for the case when the plate is located away from the stop.

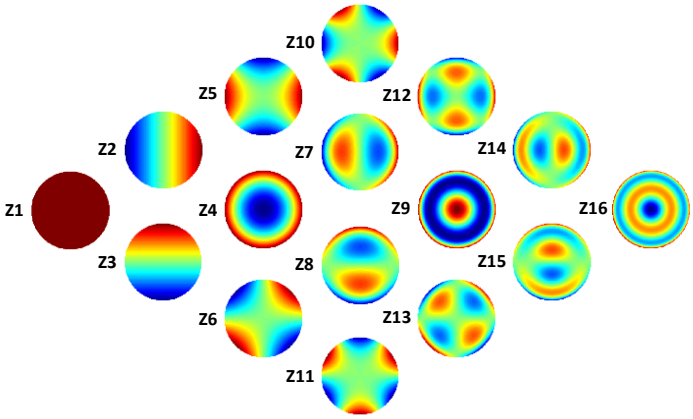

Fig. 2. Fringe Zernike polynomial set through 6th order in wavefront expansion. The set includes Z1 (piston), Z2/3 (tilt), Z4 (defocus), Z5/6 (astigmatism), Z7/8 (coma), Z9 (spherical aberration), Z10/11 (elliptical coma or trefoil), Z12/13 (oblique spherical aberration or secondary astigmatism), Z14/15 (fifth order aperture coma or secondary coma), and Z16 (fifth order spherical aberration or secondary spherical aberration). The φ-polynomials to be explored include Z5/6, Z7/8, Z10/11, Z12/13, and Z14/15.

3.1 Zernike astigmatism

In order of increasing radial dependence, the first freeform overlay term to consider is astigmatism. In optical metrology terminology, Zernike astigmatism (Fringe polynomial terms Z_5 and Z_6) is given by

$$\left(z_5\ z_6\right)\begin{pmatrix} Z_5 \\ Z_6 \end{pmatrix} = \left(z_5\ z_6\right)\begin{pmatrix} \rho^2\cos\left(2\phi\right) \\ \rho^2\sin\left(2\phi\right) \end{pmatrix}, \tag{3}$$

where z_5 and z_6 are the coefficient values for the astigmatism term, ρ is the normalized radial coordinate, and ϕ represents the azimuthal angle on the surface. In optical testing the Fringe Zernike set is described in a right-handed coordinate system with ϕ measured counter-clockwise from the $\hat{x}-$axis. The magnitude, ${}_{FF}\left|z_{5/6}\right|$, and orientation, ${}_{FF}\xi_{5/6}^{Test}$, of the freeform Zernike astigmatism overlay is calculated from the coefficients as

$${}_{FF}\left|z_{5/6}\right| = \sqrt{z_5^2 + z_6^2}, \tag{4}$$

#217287 - $15.00 USD Received 18 Jul 2014; revised 12 Sep 2014; accepted 22 Sep 2014; published 20 Oct 2014

$$ {}_{FF}\xi_{5/6}^{Test} = \frac{1}{2}\tan^{-1}\left(\frac{z_6}{z_5}\right), \tag{5} $$

where the superscript *Test* denotes the optical testing coordinate system [15].

Zernike astigmatism is introduced into the vector multiplication environment of NAT with the following observation,

$$ \text{if } \vec{\rho} = \rho\begin{pmatrix}\sin(\phi)\\ \cos(\phi)\end{pmatrix}, \quad \text{then } \vec{\rho}^{\,2} = \rho^2\begin{pmatrix}\sin(2\phi)\\ \cos(2\phi)\end{pmatrix}, \tag{6} $$

where to be consistent with commercial optical raytrace programs, a right-handed coordinate system is employed with ϕ measured clockwise from the $\hat{y}-$axis when looking towards the $-\hat{z}$ direction. To implement a coordinate system for the overlay term that is consistent with its generated aberration field within the conventions of NAT, the orientation in Eq. (5) is modified. A new orientation, ${}_{FF}\xi_{5/6}$, is defined that is displayed in Fig. 3, and given by

$$ {}_{FF}\xi_{5/6} = \frac{\pi}{2} - \frac{1}{2}\tan^{-1}\left(\frac{z_6}{z_5}\right). \tag{7} $$

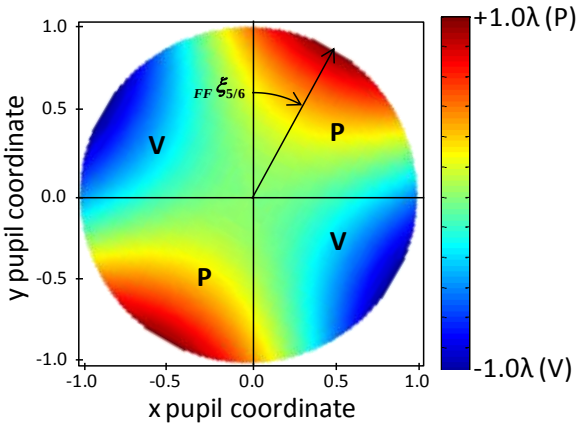

Fig. 3. Surface map describing the freeform Zernike overlay for astigmatism on an optical surface over the full aperture. The error is quantified by its magnitude ${}_{FF}|z_{5/6}|$ and its orientation ${}_{FF}\xi_{5/6}$ that is measured clockwise with respect to the $\hat{y}-$axis. P and V denote where the surface error is a peak rather than a valley.

From the vector pupil dependence in Eq. (6), it is deduced that the astigmatism overlay will induce field constant astigmatism, which is predicted by NAT (see Eqs. (4.14) and (4.16) of [4]), when the optical surface is placed at the stop or pupil. Based on this observation, it is added to the total aberration field as

$$ W_{Stop} = \frac{1}{2}\left({}_{FF}\vec{B}_{222}^{2} \bullet \vec{\rho}^{\,2}\right), \tag{8} $$

where ${}_{FF}\vec{B}_{222}^{2}$ is a two-dimensional vector that describes the magnitude and orientation of the astigmatic overlay that is related to the overall Zernike astigmatism by

$$ {}_{FF}\vec{B}_{222}^{2} \equiv 2(n'-n)\,{}_{FF}|z_{5/6}|\exp\left(i2\,{}_{FF}\xi_{5/6}\right), \tag{9} $$

#217287 - $15.00 USD Received 18 Jul 2014; revised 12 Sep 2014; accepted 22 Sep 2014; published 20 Oct 2014

where n and n' are the indices of refraction before and after the optical surface that in the case of a mirror would be –1.

If a surface with a Zernike astigmatism overlay is now placed away from the stop, the beam footprint for an off-axis field angle will begin to displace across the surface resulting in the creation of a number of field dependent terms. Replacing $\vec{\rho}$ with $\vec{\rho}'+\Delta\vec{h}$ in Eq. (8), expanding the pupil dependence, and simplifying leads to a specific set of additive terms for the wavefront expansion when a Zernike astigmatism surface is located away from the stop,

$$\begin{aligned} W_{Not\ Stop} &= \frac{1}{2}\left[{}_{FF}\vec{B}^2_{222} \bullet \left(\vec{\rho}'+\Delta\vec{h}\right)^2 \right] \\ &= \frac{1}{2}\left[{}_{FF}\vec{B}^2_{222} \bullet \vec{\rho}^{\,2} + 2\,{}_{FF}\vec{B}^2_{222} \bullet \Delta\vec{h}\,\vec{\rho} + {}_{FF}\vec{B}^2_{222} \bullet \Delta\vec{h}^{\,2} \right], \end{aligned} \tag{10}$$

where the primes on the pupil coordinate have been dropped from the final expression.

To map the impact of these additive terms on the overall field dependent wave aberration expansion of an optical system, the pupil dependence needs to be converted into existing aberration types. To this end, an additional vector operation, introduced in [4], is used,

$$\vec{A} \bullet \vec{B}\vec{C} = \vec{A}\vec{B}^* \bullet \vec{C}, \tag{11}$$

where $\vec{B}^*$ is a conjugate vector with the standard properties of a conjugate variable in the mathematics of complex numbers,

$$\vec{B}^* = \left|\vec{B}\right| \exp\left(-i\beta\right) = -B_x\hat{x} + B_y\hat{y}. \tag{12}$$

By applying the vector identity of Eq. (11), Eq. (10) takes the form

$$W_{Not\ Stop} = \frac{1}{2}\left[{}_{FF}\vec{B}^2_{222} \bullet \vec{\rho}^{\,2} + 2\,{}_{FF}\vec{B}^2_{222}\Delta\vec{h}^* \bullet \vec{\rho} + {}_{FF}\vec{B}^2_{222} \bullet \Delta\vec{h}^{\,2} \right]. \tag{13}$$

In Eq. (13) two additional field dependent aberration terms are generated in addition to the anticipated field constant astigmatism term. The second and third terms, however, are a tilt and piston that do not affect the image quality but affect the mapping and phase. Here we are focusing on image quality; therefore, these terms will not be directly addressed for this or any subsequent Zernike overlay terms. In this case, the only image degrading aberration is field constant astigmatism that is independent of where the Zernike astigmatism overlay is located with respect to the stop. A magnitude and orientation plot for the field constant astigmatism contribution is illustrated in Fig. 4. Since the aberration has no dependence on the field vector, the magnitude and orientation are the same everywhere throughout the field.

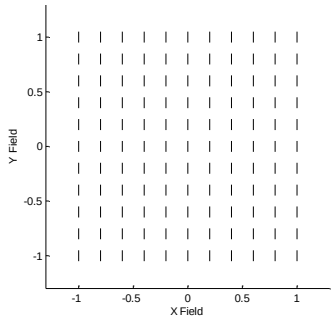

Fig. 4. The characteristic field dependence of field constant astigmatism that is generated by a Zernike astigmatism overlay on an optical surface in an optical system. This induced aberration is independent of stop position.

#217287 - $15.00 USD Received 18 Jul 2014; revised 12 Sep 2014; accepted 22 Sep 2014; published 20 Oct 2014

In order to account for freeform surfaces, the field constant astigmatism contribution can extend the existing concepts of NAT that were introduced in [4] by redefining the field constant astigmatic term of NAT, $\vec{B}_{222}^{2}$, as

$$\vec{B}_{222}^{2} = {}_{ALIGN}\vec{B}_{222}^{2} + \sum_{j=1}^{N} {}_{FF}\vec{B}_{222,j}^{2}, \tag{14}$$

where the summation and index *j* has been introduced to generalize the result to include a multi-element optical system where a Zernike astigmatism overlay may exist on multiple, independent surfaces and ${}_{ALIGN}\vec{B}_{222}^{2}$ defines the existing astigmatic component that may result from a misalignment. The misalignment may include a tilt and/or decenter of any optical component including the surfaces with a Zernike astigmatism overlay. From the definition of $\vec{B}_{222}^{2}$ in Eq. (14), the conventional strategies of NAT can be applied to solve for the nodal properties of the astigmatic aberration field when a Zernike astigmatism overlay is placed on an optical surface of a multi-element optical system.

3.2 Zernike coma

The next freeform overlay term in order of pupil dependence is Zernike coma (Fringe polynomial terms Z_7 and Z_8) that, in optical metrology terminology, is written as

$$\begin{pmatrix} z_7 & z_8 \end{pmatrix}\begin{pmatrix} Z_7 \\ Z_8 \end{pmatrix} = \begin{pmatrix} z_7 & z_8 \end{pmatrix}\begin{pmatrix} 3\rho^3\cos(\phi) - 2\rho\cos(\phi) \\ 3\rho^3\sin(\phi) - 2\rho\sin(\phi) \end{pmatrix}, \tag{15}$$

where z_7 and z_8 are the coefficient values for the coma term. Within this term there is cubic aperture (ρ^3) coma term and a linear aperture (ρ) tilt term. The tilt term is inherently built into Zernike coma to minimize the RMS WFE of the aberration polynomial over the aperture, a property of the Zernike polynomial set [10]. In order to generate coma that can be introduced in the vector multiplication environment of NAT, an adjusted Zernike coma is used that combines both Zernike coma and Zernike tilt and is written as

$$\begin{pmatrix} z_7 & z_8 \end{pmatrix}\begin{pmatrix} Z_7^{Adj} \\ Z_8^{Adj} \end{pmatrix} = \begin{pmatrix} z_7 & z_8 \end{pmatrix}\begin{pmatrix} Z_7 + 2Z_2 \\ Z_8 + 2Z_3 \end{pmatrix} = \begin{pmatrix} z_7 & z_8 \end{pmatrix}\begin{pmatrix} 3\rho^3\cos(\phi) \\ 3\rho^3\sin(\phi) \end{pmatrix}. \tag{16}$$

Similar to Zernike astigmatism, the magnitude, ${}_{FF}|z_{7/8}|$, and orientation, ${}_{FF}\xi_{7/8}$, of the freeform, adjusted Zernike coma overlay term is then calculated from the coefficients as

$${}_{FF}|z_{7/8}| = \sqrt{(z_7)^2 + (z_8)^2}, \tag{17}$$

$${}_{FF}\xi_{7/8} = \frac{\pi}{2} - \tan^{-1}\left(\frac{z_8}{z_7}\right), \tag{18}$$

where the orientation in Eq. (18) creates an orientation consistent within the conventions of NAT. The overlay term in Eq. (16) is linked to the vector multiplication environment of NAT with the following observation,

$$\textit{if } \vec{\rho} = \rho\begin{pmatrix} \sin(\phi) \\ \cos(\phi) \end{pmatrix}, \quad \textit{then } (\vec{\rho}\bullet\vec{\rho})\vec{\rho} = \rho^3\begin{pmatrix} \sin(\phi) \\ \cos(\phi) \end{pmatrix}, \tag{19}$$

#217287 - $15.00 USD Received 18 Jul 2014; revised 12 Sep 2014; accepted 22 Sep 2014; published 20 Oct 2014

where a right-handed coordinate system is employed with ϕ measured clockwise from the $\hat{y}-$axis. From the vector pupil dependence in Eq. (19), it is deduced that the overlay will induce field constant coma, which is predicted by NAT (see Eq. (4.5) of [4]), when located at the stop surface and is added to the total aberration field as

$$W_{Stop} = \left({}_{FF}\vec{A}_{131} \bullet \vec{\rho} \right)\left(\vec{\rho} \bullet \vec{\rho} \right), \tag{20}$$

where ${}_{FF}\vec{A}_{131}$ is a two-dimensional vector that describes the magnitude and orientation of the Zernike coma overlay, which is related to the overall Zernike coma by

$${}_{FF}\vec{A}_{131} \equiv 3\left(n' - n \right)_{FF}\left| z_{7/8} \right| \exp\left(i\,{}_{FF}\xi_{7/8} \right). \tag{21}$$

Now replacing $\vec{\rho}$ with $\vec{\rho}' + \Delta\vec{h}$ in Eq. (20), expanding the pupil dependence, and simplifying leads to a specific set of additive terms for the wavefront expansion when a surface with a Zernike coma overlay is located away from the stop,

$$\begin{aligned} W_{Not\ Stop} &= \left[{}_{FF}\vec{A}_{131} \bullet \left(\vec{\rho}' + \Delta\vec{h} \right) \right]\left[\left(\vec{\rho}' + \Delta\vec{h} \right) \bullet \left(\vec{\rho}' + \Delta\vec{h} \right) \right] \\ &= \begin{bmatrix} \left({}_{FF}\vec{A}_{131} \bullet \vec{\rho} \right)\left(\vec{\rho} \bullet \vec{\rho} \right) + {}_{FF}\vec{A}_{131}\Delta\vec{h} \bullet \vec{\rho}^{2} + 2\left({}_{FF}\vec{A}_{131} \bullet \Delta\vec{h} \right)\left(\vec{\rho} \bullet \vec{\rho} \right) \\ +2\left(\Delta\vec{h} \bullet \Delta\vec{h} \right)\left({}_{FF}\vec{A}_{131} \bullet \vec{\rho} \right) + \vec{A}^{*}_{131}\Delta\vec{h}^{2} \bullet \vec{\rho} + \left({}_{FF}\vec{A}_{131} \bullet \Delta\vec{h} \right)\left(\Delta\vec{h} \bullet \Delta\vec{h} \right) \end{bmatrix}, \end{aligned} \tag{22}$$

where the primes on the pupil coordinate have been dropped from the final expression and the vector identity introduced in [4],

$$2\left(\vec{A} \bullet \vec{B} \right)\left(\vec{A} \bullet \vec{C} \right) = \left(\vec{A} \bullet \vec{A} \right)\left(\vec{B} \bullet \vec{C} \right) + \vec{A}^{2} \bullet \vec{B}\vec{C}, \tag{23}$$

is used along with Eq. (11) to convert the pupil dependence into existing aberration types. As can be seen from Eq. (22), five additional field dependent aberration terms are generated in addition to the anticipated field constant coma term. The first term, which is field constant, can extend the existing concepts of NAT by redefining the field constant coma term, $\vec{A}_{131}$, as

$$\vec{A}_{131} = {}_{ALIGN}\vec{A}_{131} - \sum_{j=1}^{N} {}_{FF}\vec{A}_{131,j}, \tag{24}$$

where ${}_{ALIGN}\vec{A}_{131}$ is any comatic contribution from a misalignment. The second term of Eq. (22) is recognized to be an astigmatic term based on the $\vec{\rho}^{2}$ aperture dependence. When Eq. (1) is used to replace $\Delta\vec{h}$ in the astigmatic term of Eq. (22), it becomes

$${}_{FF}\vec{A}_{131}\Delta\vec{h} \bullet \vec{\rho}^{2} = \left(\frac{\bar{y}_j}{y_j} \right){}_{FF}\vec{A}_{131,j}\vec{H} \bullet \vec{\rho}^{2}. \tag{25}$$

Equation (25) is a form of field asymmetric, field linear astigmatism that was first seen in the derivation for the nodal structure of third order (fourth order in wavefront) astigmatism by Thompson [4, 16]. This contribution extends the field linear astigmatism contribution of NAT, $\vec{A}_{222}$, by redefining $\vec{A}_{222}$ as

$$\vec{A}_{222} = {}_{ALIGN}\vec{A}_{222} - \sum_{j=1}^{N}\left(\frac{\bar{y}_j}{y_j} \right){}_{FF}\vec{A}_{131,j}, \tag{26}$$

#217287 - $15.00 USD Received 18 Jul 2014; revised 12 Sep 2014; accepted 22 Sep 2014; published 20 Oct 2014

where ${}_{ALIGN}\vec{A}_{222}$ defines the existing astigmatic component that may result from a misalignment. The third term of Eq. (22) is recognized to be a medial field curvature term based on the $(\vec{\rho}\bullet\vec{\rho})$ aperture dependence and when $\Delta\vec{h}$ is replaced in it, it takes the form

$$2\left({}_{FF}\vec{A}_{131}\bullet\Delta\vec{h}\right)(\vec{\rho}\bullet\vec{\rho}) = 2\left(\frac{\bar{y}_j}{y_j}\right)\left({}_{FF}\vec{A}_{131}\bullet\vec{H}\right)(\vec{\rho}\bullet\vec{\rho}). \tag{27}$$

Equation (27) is now recognized as a form of field curvature, seen in the derivation for the nodal structure of third order medial field curvature by Thompson [4], that yields a tilted focal surface relative to the Gaussian image plane and extends the field linear, medial field curvature contribution of NAT, $\vec{A}_{220_M}$, by redefining $\vec{A}_{220_M}$ as

$$\vec{A}_{220_M} = {}_{ALIGN}\vec{A}_{220_M} - \sum_{j=1}^{N}\left(\frac{\bar{y}_j}{y_j}\right){}_{FF}\vec{A}_{131,j}, \tag{28}$$

where ${}_{ALIGN}\vec{A}_{220_M}$ defines the existing field linear, medial field curvature component that may result from a misalignment. The process of extending the existing concepts of NAT to the aberration terms generated by a Zernike coma overlay is summarized in Table 1 where the aberration terms from Eq. (22) are displayed in column one with $\Delta\vec{h}$ replaced by its form using Eq. (1), column two displays the NAT analog term that has the same field and pupil behavior as the generated terms in column one, and column three displays how the NAT analog term is extended to include both the misalignment and freeform overlay components.

Table 1. Image Degrading Aberration Terms That Are Generated by a Zernike Coma Overlay and How the Terms Link to Existing Concepts of NAT and Extend the Theory to Include Freeform Surfaces

Aberration Terms for a Zernike Coma Overlay	NAT Analog[a]	Extension of NAT for freeform surfaces
$\left({}_{FF}\vec{A}_{131,j}\bullet\vec{\rho}\right)(\vec{\rho}\bullet\vec{\rho})$	$-\left(\vec{A}_{131}\bullet\vec{\rho}\right)(\vec{\rho}\bullet\vec{\rho})$	$\vec{A}_{131} = {}_{ALIGN}\vec{A}_{131} - \sum_{j=1}^{N}{}_{FF}\vec{A}_{131,j}$
$\left(\frac{\bar{y}_j}{y_j}\right){}_{FF}\vec{A}_{131,j}\vec{H}\bullet\vec{\rho}^2$	$\frac{1}{2}\left(-2\vec{A}_{222}\vec{H}\bullet\vec{\rho}^2\right)$	$\vec{A}_{222} = {}_{ALIGN}\vec{A}_{222} - \sum_{j=1}^{N}\left(\frac{\bar{y}_j}{y_j}\right){}_{FF}\vec{A}_{131,j}$
$2\left(\frac{\bar{y}_j}{y_j}\right)\left({}_{FF}\vec{A}_{131,j}\bullet\vec{H}\right)(\vec{\rho}\bullet\vec{\rho})$	$-2\left(\vec{A}_{220_M}\bullet\vec{H}\right)(\vec{\rho}\bullet\vec{\rho})$	$\vec{A}_{220_M} = {}_{ALIGN}\vec{A}_{220_M} - \sum_{j=1}^{N}\left(\frac{\bar{y}_j}{y_j}\right){}_{FF}\vec{A}_{131,j}$

[a]From J. Opt. Soc. Am. A **22**, 1389-1401 (2005).

The magnitude and orientation plots of the aberration terms generated by a Zernike coma overlay, summarized in Table 1, are depicted throughout the field in Figs. 5(a)–5(c). In Fig. 5(a), the field constant comatic contribution from a Zernike coma overlay is displayed. The magnitude and orientation are the same everywhere throughout the field and are governed by the vector describing the overlay term, ${}_{FF}\vec{A}_{131}$. In Fig. 5(b), the astigmatic contribution from a Zernike coma overlay away from the stop is displayed. As can be seen from the line images, the aberration is asymmetric with field while increasing linearly from a single node. Lastly, in Fig. 5(c), the medial field curvature contribution is displayed. This form of field curvature increases linearly with field in the direction of the vector describing the overlay term, ${}_{FF}\vec{A}_{131}$.

#217287 - $15.00 USD Received 18 Jul 2014; revised 12 Sep 2014; accepted 22 Sep 2014; published 20 Oct 2014

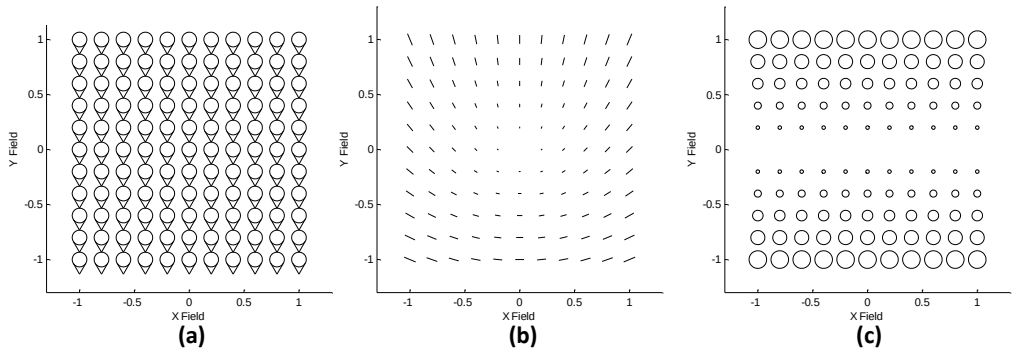

Fig. 5. The characteristic field dependence of (a) field constant coma, (b) field asymmetric, field linear astigmatism, and (c) field linear, medial field curvature that is generated by a Zernike coma overlay on an optical surface away from the stop surface.

3.3 Zernike trefoil (elliptical coma)

The next freeform overlay term is Zernike trefoil (Fringe polynomial terms Z_{10} and Z_{11}), which has been previously discussed by Fuerschbach et al. [7] and is included here again for completeness. Zernike trefoil has the same pupil dependence as coma but a higher order azimuthal dependence and, in optical metrology terminology, is written as

$$\begin{pmatrix} z_{10} & z_{11} \end{pmatrix} \begin{pmatrix} Z_{10} \\ Z_{11} \end{pmatrix} = \begin{pmatrix} z_{10} & z_{11} \end{pmatrix} \begin{pmatrix} \rho^3 \cos(3\phi) \\ \rho^3 \sin(3\phi) \end{pmatrix}, \tag{29}$$

where z_{10} and z_{11} are the coefficient values for the trefoil term. The magnitude, ${}_{FF}\left|z_{10/11}\right|$, and orientation, ${}_{FF}\xi_{10/11}$, of the Zernike trefoil is then calculated from the coefficients as

$${}_{FF}\left|z_{10/11}\right| = \sqrt{z_{10}^2 + z_{11}^2}, \tag{30}$$

$${}_{FF}\xi_{10/11} = \frac{\pi}{2} - \frac{1}{3}\tan^{-1}\left(\frac{z_{11}}{z_{10}}\right). \tag{31}$$

The overlay term in Eq. (29) is linked to the vector multiplication environment of NAT with the following observation,

$$\textit{if } \vec{\rho} = \rho \begin{pmatrix} \sin(\phi) \\ \cos(\phi) \end{pmatrix}, \quad \textit{then } \vec{\rho}^3 = \rho^3 \begin{pmatrix} \sin(3\phi) \\ \cos(3\phi) \end{pmatrix}, \tag{32}$$

where a right-handed coordinate system is employed with ϕ measured clockwise from the $\hat{y}-$axis. From the vector pupil dependence in Eq. (32), it is deduced that the trefoil deformation will induce field constant, elliptical coma, which is predicted by NAT (see Eq. (19) of [17]), when located at the stop surface and is added to the total aberration field as

$$W_{Stop} = \frac{1}{4}\left({}_{FF}\vec{C}^{3}_{333} \bullet \vec{\rho}^3 \right), \tag{33}$$

where ${}_{FF}\vec{C}^{3}_{333}$ is a two-dimensional vector that describes the magnitude and orientation of field constant elliptical coma, which is related to the overall Zernike trefoil by

$${}_{FF}\vec{C}^{3}_{333} \equiv 4(n'-n)\,{}_{FF}\left|z_{10/11}\right| \exp\left(i3\,{}_{FF}\xi_{10/11}\right). \tag{34}$$

#217287 - $15.00 USD Received 18 Jul 2014; revised 12 Sep 2014; accepted 22 Sep 2014; published 20 Oct 2014

Now replacing $\vec{\rho}$ with $\vec{\rho}'+\Delta\vec{h}$ in Eq. (33), expanding the pupil dependence, and simplifying leads to a specific set of additive terms for the wavefront expansion when a surface with a Zernike trefoil overlay is located away from the stop,

$$\begin{aligned} W_{Not\ Stop} &= \frac{1}{4}\left[{}_{FF}\vec{C}^{3}_{333}\bullet\left(\vec{\rho}'+\Delta\vec{h}\right)^{3}\right] \\ &= \frac{1}{4}\left[\begin{array}{l} {}_{FF}\vec{C}^{3}_{333}\bullet\vec{\rho}^{3}+3\,{}_{FF}\vec{C}^{3}_{333}\Delta\vec{h}^{*}\bullet\vec{\rho}^{2} \\ +3\,{}_{FF}\vec{C}^{3}_{333}\Delta\vec{h}^{*2}\bullet\vec{\rho}+{}_{FF}\vec{C}^{3}_{333}\bullet\Delta\vec{h}^{3} \end{array}\right], \end{aligned} \tag{35}$$

where the primes on the pupil coordinate have been dropped from the final expression and the vector identity in Eq. (11) is used to convert the pupil dependence into existing aberration types. In Eq. (35), three additional field dependent aberration terms are generated in addition to the anticipated field constant elliptical coma (trefoil) term. Following the method outlined for the Zernike coma overlay, Table 2 displays the image degrading aberration terms generated by the Zernike trefoil overlay with $\Delta\vec{h}$ replaced in each term and shows how each term links to existing concepts of NAT and extends the theory to account for freeform surfaces.

Table 2. Image Degrading Aberration Terms That Are Generated by a Zernike Elliptical Coma Overlay and How the Terms Link to Existing Concepts of NAT and Extend the Theory to Include Freeform Surfaces

Aberration Terms for a Zernike Trefoil Overlay	NAT Analog[a,b]	Extension of NAT for freeform surfaces
$\frac{1}{4}\,{}_{FF}\vec{C}^{3}_{333,j}\bullet\vec{\rho}^{3}$	$-\frac{1}{4}\vec{C}^{3}_{333}\bullet\vec{\rho}^{3}$	$\vec{C}^{3}_{333}={}_{ALIGN}\vec{C}^{3}_{333}-\sum_{j=1}^{N}{}_{FF}\vec{C}^{3}_{333,j}$
$\frac{3}{4}\left(\frac{\bar{y}_j}{y_j}\right){}_{FF}\vec{C}^{3}_{333,j}\vec{H}^{*}\bullet\vec{\rho}^{2}$	$\frac{1}{2}\left(-\vec{C}^{3}_{422}\vec{H}^{*}\bullet\vec{\rho}^{2}\right)$	$\vec{C}^{3}_{422}={}_{ALIGN}\vec{C}^{3}_{422}-\frac{3}{2}\sum_{j=1}^{N}\left(\frac{\bar{y}_j}{y_j}\right){}_{FF}\vec{C}^{3}_{333,j}$

[a]From J. Opt. Soc. Am. A **27**, 1490-1504 (2010)
[b]From J. Opt. Soc. Am. A **28**, 821-836 (2011).

In Table 2, it can be seen that the field constant elliptical coma term pairs with ${}_{ALIGN}\vec{C}^{3}_{333}$ which is a fifth order (sixth order in wavefront) misalignment induced aberration component. Normally, since ${}_{ALIGN}\vec{C}^{3}_{333}$ is a cubic vector, this contribution is small and dominated by lower order misalignment contributions. However, with the use of freeform overlays, particularly any overlay of equal or higher order than Zernike trefoil, the fifth order aberration space and their misalignment induced aberration components like $\vec{C}^{3}_{333}$ can be roughly equal to or greater than the third order misalignment induced aberration components of NAT.

The second term from Eq. (35) is seen to be an astigmatic term based on the $\vec{\rho}^{2}$ aperture dependence and it is a form of field linear astigmatism that was first seen in the derivation for the nodal structure of field quartic fifth order astigmatism by Thompson [18], and reported in Table 2 (second row, second column). Subsequently, this linear astigmatism was isolated by Fuerschbach et al. [7] and linked to an astigmatic form that may appear when three point mount error exists on a surface away from the stop surface.

The magnitude and orientation plots of the aberration terms generated by a Zernike trefoil overlay, summarized in Table 2, are depicted throughout the field in Figs. 6(a) and 6(b). In Fig. 6(a), the field constant elliptical coma contribution from a Zernike trefoil overlay is displayed. The magnitude and orientation are the same everywhere throughout the field and are governed by the vector describing the overlay term, ${}_{FF}\vec{C}^{3}_{333}$. In Fig. 6(b), the astigmatic

#217287 - $15.00 USD Received 18 Jul 2014; revised 12 Sep 2014; accepted 22 Sep 2014; published 20 Oct 2014

contribution from a Zernike trefoil overlay away from the stop is displayed. The aberration is of the same order as field asymmetric, field linear astigmatism but it depends on the conjugate vector so it takes on a different orientation throughout the field. This form of astigmatic field dependence was first reported in the literature by Stacy [19], but its analytical origin remained unexplained until Fuerschbach et al. [7].

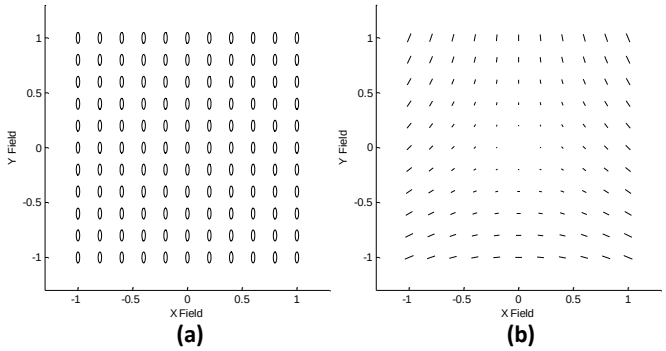

Fig. 6. The characteristic field dependence of (a) field constant elliptical coma, (b) field conjugate, field linear astigmatism, which is generated by a Zernike elliptical coma overlay on an optical surface away from the stop surface.

3.4 Zernike oblique spherical aberration

Moving to the next pupil order, the next freeform overlay term is Zernike oblique spherical (Fringe polynomial terms Z_{12} and Z_{13}) that, in optical metrology terminology, is written as

$$\begin{pmatrix} z_{12} & z_{13} \end{pmatrix}\begin{pmatrix} Z_{12} \\ Z_{13} \end{pmatrix} = \begin{pmatrix} z_{12} & z_{13} \end{pmatrix}\begin{pmatrix} 4\rho^4\cos(2\phi) - 3\rho^2\cos(2\phi) \\ 4\rho^4\sin(2\phi) - 3\rho^2\sin(2\phi) \end{pmatrix}, \tag{36}$$

where z_{12} and z_{13} are the coefficient values for the oblique spherical term. Within this term there is a quartic aperture (ρ^4) oblique spherical aberration term and a quadratic aperture (ρ^2) astigmatism term. Similar to the case of Zernike coma, there is an included astigmatic term to minimize the RMS WFE of the oblique spherical aberration term. In order to generate oblique spherical aberration that can be introduced in the vector multiplication environment of NAT, an adjusted Zernike oblique spherical aberration is used that combines both Zernike oblique spherical aberration and Zernike astigmatism and is written as

$$\begin{pmatrix} z_{12} & z_{13} \end{pmatrix}\begin{pmatrix} Z_{12}^{Adj} \\ Z_{13}^{Adj} \end{pmatrix} = \begin{pmatrix} z_{12} & z_{13} \end{pmatrix}\begin{pmatrix} Z_{12} + 3Z_5 \\ Z_{12} + 3Z_6 \end{pmatrix} = \begin{pmatrix} z_{12} & z_{13} \end{pmatrix}\begin{pmatrix} 4\rho^4\cos(2\phi) \\ 4\rho^4\sin(2\phi) \end{pmatrix}. \tag{37}$$

The magnitude, ${}_{FF}|z_{12/13}|$, and orientation, ${}_{FF}\xi_{12/13}$, of the freeform, adjusted Zernike oblique spherical aberration overlay term is then calculated from the coefficients as

$${}_{FF}|z_{12/13}| = \sqrt{(z_{12})^2 + (z_{13})^2}, \tag{38}$$

$${}_{FF}\xi_{12/13} = \frac{\pi}{2} - \frac{1}{2}\tan^{-1}\left(\frac{z_{13}}{z_{12}}\right). \tag{39}$$

The overlay term in Eq. (37) is linked to the vector multiplication environment of NAT with the following observation,

#217287 - $15.00 USD Received 18 Jul 2014; revised 12 Sep 2014; accepted 22 Sep 2014; published 20 Oct 2014

$$if\ \vec{\rho} = \rho\begin{pmatrix}\sin(\phi)\\ \cos(\phi)\end{pmatrix},\quad then\ (\vec{\rho}\bullet\vec{\rho})\vec{\rho}^{\,2} = \rho^4\begin{pmatrix}\sin(2\phi)\\ \cos(2\phi)\end{pmatrix}, \tag{40}$$

where a right-handed coordinate system is employed with ϕ measured clockwise from the $\hat{y}-$axis. From the vector pupil dependence in Eq. (40), it is deduced that the oblique spherical overlay will induce field constant, oblique spherical aberration, which is predicted by NAT (see Eq. (14) of [20]), when located at the stop surface and is added to the total aberration field as

$$W_{Stop} = \frac{1}{2}\left({}_{FF}\vec{B}^{2}_{242}\bullet\vec{\rho}^{\,2}\right)(\vec{\rho}\bullet\vec{\rho}), \tag{41}$$

where ${}_{FF}\vec{B}^{2}_{242}$ is a two-dimensional vector that describes the magnitude and orientation of field constant oblique spherical aberration, which relates to adjusted Zernike oblique spherical aberration by

$${}_{FF}\vec{B}^{2}_{242} \equiv 8(n'-n)\,{}_{FF}\left|z_{12/13}\right|\exp\left(i2\,{}_{FF}\xi_{12/13}\right). \tag{42}$$

Now replacing $\vec{\rho}$ with $\vec{\rho}'+\Delta\vec{h}$ in Eq. (41), expanding the pupil dependence, and simplifying leads to a specific set of additive terms for the wavefront expansion when a surface with a Zernike oblique spherical aberration overlay is located away from the stop,

$$\begin{aligned} W_{Not\ Stop} &= \frac{1}{2}\left[{}_{FF}\vec{B}^{2}_{242}\bullet\left(\vec{\rho}'+\Delta\vec{h}\right)^2\right]\left[\left(\vec{\rho}'+\Delta\vec{h}\right)\bullet\left(\vec{\rho}'+\Delta\vec{h}\right)\right] \\ &= \frac{1}{2}\begin{bmatrix} \left({}_{FF}\vec{B}^{2}_{242}\bullet\vec{\rho}^{\,2}\right)(\vec{\rho}\bullet\vec{\rho}) + 3\left({}_{FF}\vec{B}^{2}_{242}\Delta\vec{h}^{*}\bullet\vec{\rho}\right)(\vec{\rho}\bullet\vec{\rho}) + {}_{FF}\vec{B}^{2}_{242}\Delta\vec{h}\bullet\vec{\rho}^{\,3} \\ +3\left(\Delta\vec{h}\bullet\Delta\vec{h}\right)\left({}_{FF}\vec{B}^{2}_{242}\bullet\vec{\rho}^{\,2}\right) + 3\left({}_{FF}\vec{B}^{2}_{242}\bullet\Delta\vec{h}^{2}\right)(\vec{\rho}\bullet\vec{\rho}) \\ +2\left({}_{FF}\vec{B}^{2}_{242}\bullet\Delta\vec{h}^{2}\right)\left(\Delta\vec{h}\bullet\vec{\rho}\right) + 2\left(\Delta\vec{h}\bullet\Delta\vec{h}\right)\left({}_{FF}\vec{B}^{2}_{242}\Delta\vec{h}^{*}\bullet\vec{\rho}\right) \\ +\left(\Delta\vec{h}\bullet\Delta\vec{h}\right)\left({}_{FF}\vec{B}^{2}_{242}\bullet\Delta\vec{h}^{2}\right) \end{bmatrix}, \end{aligned} \tag{43}$$

where the primes on the pupil coordinate have been dropped from the final expression and two vector identities introduced in [4, 21],

$$2\left(\vec{A}\bullet\vec{B}\right)\left(\vec{A}^{2}\bullet\vec{C}^{2}\right) = \left(\vec{A}\bullet\vec{A}\right)\left(\vec{A}\vec{B}\bullet\vec{C}\right) + \vec{A}^{3}\bullet\vec{B}\vec{C}^{2}, \tag{44}$$

$$2\left(\vec{A}\bullet\vec{B}\right)\left(\vec{A}\vec{B}\bullet\vec{C}^{2}\right) = \left(\vec{A}\bullet\vec{A}\right)\left(\vec{B}^{2}\bullet\vec{C}\right) + \left(\vec{B}\bullet\vec{B}\right)\left(\vec{A}^{2}\bullet\vec{C}^{2}\right), \tag{45}$$

are used along with Eq. (11) to convert the pupil dependence into existing aberration types. As can be seen from Eq. (43), seven additional field dependent aberration terms are generated in addition to the anticipated field constant oblique spherical aberration term. Table 3 displays the image degrading aberration terms generated by the Zernike oblique spherical aberration overlay with $\Delta\vec{h}$ replaced in each term and shows how each term links to existing concepts of NAT and extends the theory to account for freeform surfaces. In order of decreasing pupil dependence, the first term is field constant oblique spherical aberration. The second term is identified as an elliptical coma aberration based on the $\vec{\rho}^{\,3}$ dependence, where, the elliptical coma is linear throughout the field. The third term is identified as a comatic aberration based on the $(\vec{\rho}\bullet\vec{\rho})\vec{\rho}$ dependence. The aberration field is linear with conjugate field dependence and belongs with the misalignment induced aberrations of field cubic coma. The fourth term

#217287 - $15.00 USD Received 18 Jul 2014; revised 12 Sep 2014; accepted 22 Sep 2014; published 20 Oct 2014

is a fifth order astigmatic aberration based on the $\vec{\rho}^2$ dependence where the aberration is quadratic with field from the $\left(\vec{H}\bullet\vec{H}\right)$ component; however, since this quantity is a scalar, the orientation only depends on the vector ${}_{FF}\vec{B}^2_{242,j}$ and, as a result, the orientation is constant throughout the field. The final term is a fifth order medial field curvature aberration based on the $\left(\vec{\rho}\bullet\vec{\rho}\right)$ dependence that yields a saddle shaped focal surface relative to the Gaussian image plane.

Table 3. Image Degrading Aberration Terms That Are Generated by a Zernike Oblique Spherical Aberration Overlay and How the Terms Link to Existing Concepts of NAT and Extend the Theory to Include Freeform Surfaces

Aberration Terms for a Zernike Oblique Spherical Aberration Overlay	NAT Analog[a,b,c]	Extension of NAT for freeform surfaces
$\frac{1}{2}\left({}_{FF}\vec{B}^2_{242,j}\bullet\vec{\rho}^2\right)\left(\vec{\rho}\bullet\vec{\rho}\right)$	$\frac{1}{2}\left(\vec{B}^2_{242}\bullet\vec{\rho}^2\right)\left(\vec{\rho}\bullet\vec{\rho}\right)$	$\vec{B}^2_{242} = {}_{ALIGN}\vec{B}^2_{242} + \sum_{j=1}^{N} {}_{FF}\vec{B}^2_{242,j}$
$\frac{1}{2}\left(\frac{\bar{y}_j}{y_j}\right){}_{FF}\vec{B}^2_{242,j}\vec{H}\bullet\vec{\rho}^3$	$\frac{1}{4}\left(3\vec{B}^2_{333}\vec{H}\bullet\vec{\rho}^3\right)$	$\vec{B}^2_{333} = {}_{ALIGN}\vec{B}^2_{333} + \frac{2}{3}\sum_{j=1}^{N}\left(\frac{\bar{y}_j}{y_j}\right){}_{FF}\vec{B}^2_{242,j}$
$\frac{3}{2}\left(\frac{\bar{y}_j}{y_j}\right)\left({}_{FF}\vec{B}^2_{242,j}\vec{H}^*\bullet\vec{\rho}\right)\left(\vec{\rho}\bullet\vec{\rho}\right)$	$\left(\vec{B}^2_{331_M}\vec{H}^*\bullet\vec{\rho}\right)\left(\vec{\rho}\bullet\vec{\rho}\right)$	$\vec{B}^2_{331_M} = {}_{ALIGN}\vec{B}^2_{331_M} + \frac{3}{2}\sum_{j=1}^{N}\left(\frac{\bar{y}_j}{y_j}\right){}_{FF}\vec{B}^2_{242,j}$
$\frac{3}{2}\left(\frac{\bar{y}_j}{y_j}\right)^2\left(\vec{H}\bullet\vec{H}\right)\left({}_{FF}\vec{B}^2_{242,j}\bullet\vec{\rho}^2\right)$	$\frac{1}{2}\left[3\left(\vec{H}\bullet\vec{H}\right)\left(\vec{B}^2_{422}\bullet\vec{\rho}^2\right)\right]$	$\vec{B}^2_{422} = {}_{ALIGN}\vec{B}^2_{422} + \sum_{j=1}^{N}\left(\frac{\bar{y}_j}{y_j}\right)^2{}_{FF}\vec{B}^2_{242,j}$
$\frac{3}{2}\left(\frac{\bar{y}_j}{y_j}\right)^2\left({}_{FF}\vec{B}^2_{242,j}\bullet\vec{H}^2\right)\left(\vec{\rho}\bullet\vec{\rho}\right)$	$2\left(\vec{B}^2_{420_M}\bullet\vec{H}^2\right)\left(\vec{\rho}\bullet\vec{\rho}\right)$	$\vec{B}^2_{420_M} = {}_{ALIGN}\vec{B}^2_{420_M} + \frac{3}{4}\sum_{j=1}^{N}\left(\frac{\bar{y}_j}{y_j}\right)^2{}_{FF}\vec{B}^2_{242,j}$

[a]From J. Opt. Soc. Am. A **26**, 1090-1100 (2009)
[b]From J. Opt. Soc. Am. A **27**, 1490-1504 (2010)
[c]From J. Opt. Soc. Am. A **28**, 821-836 (2011).

The magnitude and orientation plots of the aberration terms generated by a Zernike oblique spherical aberration overlay, summarized in Table 3, are depicted throughout the field in Figs. 7(a)–7(e). In Fig. 7(a), the field constant oblique spherical aberration contribution from a Zernike oblique spherical aberration overlay is displayed. The magnitude and orientation are the same everywhere throughout the field and are governed by the vector describing the overlay term, ${}_{FF}\vec{B}^2_{242}$. In Fig. 7(b), the elliptical coma contribution from a Zernike oblique spherical aberration overlay away from the stop is displayed. The field behavior of this elliptical coma term is of the same form as field asymmetric, field linear astigmatism. Figure 7(c) displays the field cubic comatic contribution where the conjugate field dependence of the aberration yields a unique orientation when compared to conventional third order field linear coma. The fifth order astigmatic contribution, Fig. 7(d), exhibits a field constant orientation while the magnitude of the aberration varies quadratically with the field vector. Lastly, Fig. 7(e), displays a fifth order medial field curvature contribution that equates to a saddle shaped focal plane as the aberration curves up in one direction and down in the other.

#217287 - $15.00 USD Received 18 Jul 2014; revised 12 Sep 2014; accepted 22 Sep 2014; published 20 Oct 2014

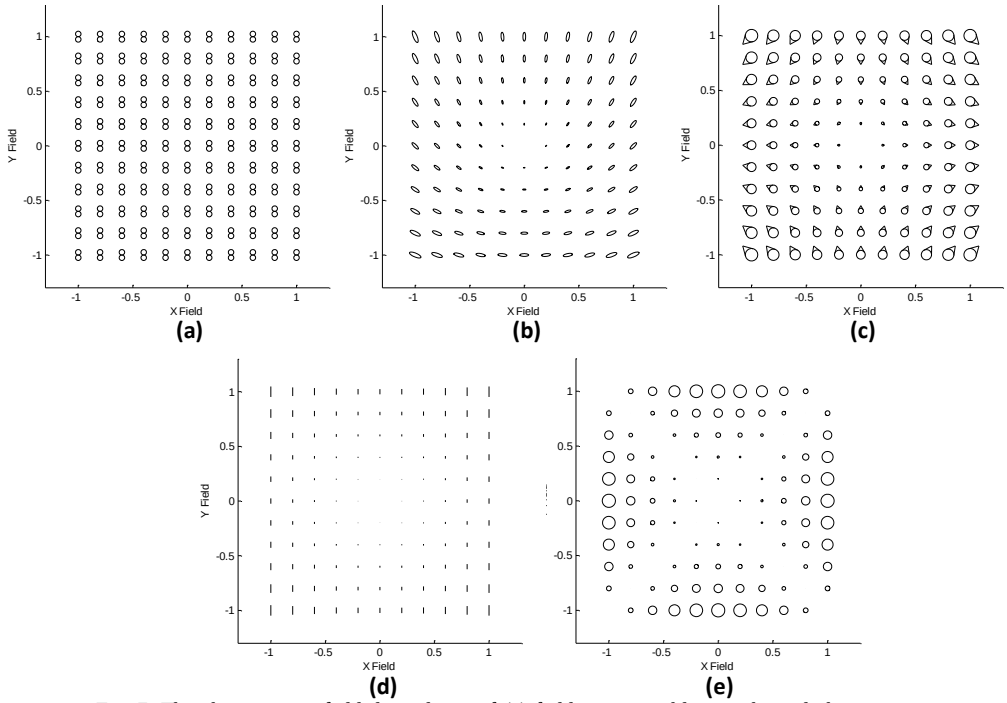

Fig. 7. The characteristic field dependence of (a) field constant oblique spherical aberration, (b) field asymmetric, field linear trefoil, (c) field conjugate, field linear coma, (d) field constant, field quadratic astigmatism, and (e) saddle shaped, field quadratic, medial field curvature that is generated by a Zernike oblique spherical aberration overlay on an optical surface away from the stop surface.

3.5 Zernike fifth order aperture coma

The next pupil order and last freeform overlay term is Zernike fifth order aperture coma (Fringe polynomial terms Z_{14} and Z_{15}) that, in optical metrology terminology, is written as

$$\left(z_{14}\ z_{15}\right)\begin{pmatrix} Z_{14} \\ Z_{15} \end{pmatrix} = \left(z_{14}\ z_{15}\right)\begin{pmatrix} 10\rho^5\cos(\phi) - 12\rho^3\cos(\phi) + 3\rho\cos(\phi) \\ 10\rho^5\sin(\phi) - 12\rho^3\sin(\phi) + 3\rho\sin(\phi) \end{pmatrix}, \qquad (46)$$

where z_{14} and z_{15} are the coefficient values for the fifth order coma term. Within this term there is a quintic aperture (ρ^5) coma term, a cubic aperture (ρ^3) coma term, and a linear aperture (ρ) tilt term to minimize the RMS WFE of the fifth order aperture coma term. To generate a fifth order aperture coma that can be introduced in the vector multiplication environment of NAT, an adjusted Zernike fifth order coma is used that combines Zernike fifth order aperture coma, Zernike coma, and Zernike tilt and is written as

$$\left(z_{14}\ z_{15}\right)\begin{pmatrix} Z_{14}^{Adj} \\ Z_{15}^{Adj} \end{pmatrix} = \left(z_{14}\ z_{15}\right)\begin{pmatrix} Z_{14} + 4Z_7 + 5Z_2 \\ Z_{15} + 4Z_8 + 5Z_3 \end{pmatrix} = \left(z_{14}\ z_{15}\right)\begin{pmatrix} 10\rho^5\cos(\phi) \\ 10\rho^5\sin(\phi) \end{pmatrix}. \qquad (47)$$

The magnitude, ${}_{FF}\left|z_{14/15}\right|$, and orientation, ${}_{FF}\xi_{14/15}$, of the freeform, adjusted Zernike fifth order aperture coma overlay term is then calculated from the coefficients as

$${}_{FF}\left|z_{14/15}\right| = \sqrt{\left(z_{14}\right)^2 + \left(z_{15}\right)^2}, \qquad (48)$$

#217287 - $15.00 USD Received 18 Jul 2014; revised 12 Sep 2014; accepted 22 Sep 2014; published 20 Oct 2014

$$ {}_{FF}\xi_{14/15} = \frac{\pi}{2} - \tan^{-1}\left(\frac{z_{15}}{z_{14}}\right). \tag{49} $$

The overlay term in Eq. (47) is linked to the vector multiplication environment of NAT with the following observation,

$$ \text{if } \vec{\rho} = \rho\begin{pmatrix}\sin(\phi)\\ \cos(\phi)\end{pmatrix}, \quad \text{then } (\vec{\rho}\bullet\vec{\rho})^2\,\vec{\rho} = \rho^5\begin{pmatrix}\sin(\phi)\\ \cos(\phi)\end{pmatrix}, \tag{50} $$

where a right-handed coordinate system is employed with ϕ measured clockwise from the $\hat{y}-$axis. From the vector pupil dependence in Eq. (50), it is deduced that the fifth order aperture coma overlay will induce field constant, fifth order aperture coma, which is predicted by NAT (see Eq. (4.7) of [17]), when located at the stop surface and is added to the total aberration field as

$$ W_{Stop} = \left({}_{FF}\vec{A}_{151}\bullet\vec{\rho}\right)(\vec{\rho}\bullet\vec{\rho})^2, \tag{51} $$

where ${}_{FF}\vec{A}_{151}$ is a two-dimensional vector describing the magnitude and orientation of field constant, fifth order aperture coma, which relates to adjusted Zernike fifth order coma by

$$ {}_{FF}\vec{A}_{151} \equiv 10(n'-n)\,{}_{FF}\left|z_{14/15}\right|\exp\left(i\,{}_{FF}\xi_{14/15}\right). \tag{52} $$

Now replacing $\vec{\rho}$ with $\vec{\rho}'+\Delta\vec{h}$ in Eq. (51), expanding the pupil dependence, and simplifying leads to a specific set of additive terms for the wavefront expansion when a surface with a Zernike fifth order aperture coma overlay is located away from the stop,

$$ \begin{aligned} W_{Not\ Stop} &= \left[{}_{FF}\vec{A}_{151}\bullet\left(\vec{\rho}'+\Delta\vec{h}\right)\right]\left[\left(\vec{\rho}'+\Delta\vec{h}\right)\bullet\left(\vec{\rho}'+\Delta\vec{h}\right)\right]^2 \\ &= \left\{\begin{array}{l} \left({}_{FF}\vec{A}_{151}\bullet\vec{\rho}\right)(\vec{\rho}\bullet\vec{\rho})^2 + 3\left({}_{FF}\vec{A}_{151}\bullet\Delta\vec{h}\right)(\vec{\rho}\bullet\vec{\rho})^2 + \left({}_{FF}\vec{A}_{151}\Delta\vec{h}^2\bullet\vec{\rho}^3\right) \\ +\left[6\left({}_{FF}\vec{A}_{151}\bullet\Delta\vec{h}\right)\Delta\vec{h} + 3\left(\Delta\vec{h}\bullet\Delta\vec{h}\right){}_{FF}\vec{A}_{151}\right]\bullet\vec{\rho}(\vec{\rho}\bullet\vec{\rho}) \\ +\left[2\left({}_{FF}\vec{A}_{151}\bullet\Delta\vec{h}\right)\Delta\vec{h}^2 + 2\left(\Delta\vec{h}\bullet\Delta\vec{h}\right){}_{FF}\vec{A}_{151}\Delta\vec{h}\right]\bullet\vec{\rho}^2 \\ +2\left({}_{FF}\vec{A}_{151}\Delta\vec{h}\bullet\vec{\rho}^2\right)(\vec{\rho}\bullet\vec{\rho}) + 6\left(\Delta\vec{h}\bullet\Delta\vec{h}\right)\left({}_{FF}\vec{A}_{151}\bullet\Delta\vec{h}\right)(\vec{\rho}\bullet\vec{\rho}) \\ +\left[\left(\Delta\vec{h}\bullet\Delta\vec{h}\right)^2{}_{FF}\vec{A}_{151} + 4\left({}_{FF}\vec{A}_{151}\bullet\Delta\vec{h}\right)\left(\Delta\vec{h}\bullet\Delta\vec{h}\right)\Delta\vec{h}\right]\bullet\vec{\rho} \\ +\left(\Delta\vec{h}\bullet\Delta\vec{h}\right)^2\left({}_{FF}\vec{A}_{151}\bullet\Delta\vec{h}\right) \end{array}\right\}, \end{aligned} \tag{53} $$

where the primes on the pupil coordinate have been dropped from the final expression and the vector identities in Eq. (11) and Eq. (23) are used to convert the pupil dependence into existing aberration types. As can be seen from Eq. (53), eleven additional field dependent aberration terms are generated in addition to the anticipated field constant fifth order aperture coma term. Table 4 displays the image degrading aberration terms generated by the Zernike fifth order aperture coma overlay with $\Delta\vec{h}$ replaced in each term and shows how each term links to existing concepts of NAT and extends the theory to account for freeform surfaces. In order of decreasing pupil dependence, the first term is field constant fifth order aperture coma. The second term is identified as medial oblique spherical aberration and it equates to a tilted medial surface for oblique spherical aberration relative to the Gaussian image plane. The third term is identified as oblique spherical aberration based on the $(\vec{\rho}\bullet\vec{\rho})\vec{\rho}^2$ dependence where the aberration is linear throughout the field. The fourth term is an elliptical coma

#217287 - $15.00 USD Received 18 Jul 2014; revised 12 Sep 2014; accepted 22 Sep 2014; published 20 Oct 2014

aberration based on the $\vec{\rho}^3$ dependence where the aberration is quadratic with field. The fifth and sixth terms are both identified as a form of coma based on the $(\vec{\rho}\bullet\vec{\rho})\vec{\rho}$ dependence and are found as a misalignment induced aberration of fifth order, field cubic coma. Likewise, the seventh and eighth terms are a form astigmatism based on the $\vec{\rho}^2$ dependence and are found as a misalignment induced aberration of fifth order astigmatism. Lastly, the ninth term is a fifth order medial field curvature term that manipulates the focal surface relative to the Gaussian image plane.

Table 4. Image Degrading Aberration Terms That Are Generated by a Zernike Fifth Order Aperture Coma Overlay and How the Terms Link to Existing Concepts of NAT and Extend the Theory to Include Freeform Surfaces

Aberration Terms for a Zernike Fifth Order Aperture Coma Overlay	NAT Analog[a,b,c]	Extension of NAT for freeform surfaces
$\left({}_{FF}\vec{A}_{151,j}\bullet\vec{\rho}\right)(\vec{\rho}\bullet\vec{\rho})^2$	$-\left(\vec{A}_{151}\bullet\vec{\rho}\right)(\vec{\rho}\bullet\vec{\rho})^2$	$\vec{A}_{151} = {}_{ALIGN}\vec{A}_{151} - \sum_{j=1}^{N} {}_{FF}\vec{A}_{151,j}$
$3\left(\frac{\bar{y}_j}{y_j}\right)\left(\vec{H}\bullet\vec{A}_{151,j}\right)(\vec{\rho}\bullet\vec{\rho})^2$	$-2\left(\vec{H}\bullet\vec{A}_{240_M}\right)(\vec{\rho}\bullet\vec{\rho})^2$	$\vec{A}_{240_M} = {}_{ALIGN}\vec{A}_{240_M} - \frac{3}{2}\sum_{j=1}^{N}\left(\frac{\bar{y}_j}{y_j}\right) {}_{FF}\vec{A}_{151,j}$
$2\left(\frac{\bar{y}_j}{y_j}\right)\left({}_{FF}\vec{A}_{151,j}\vec{H}\bullet\vec{\rho}^2\right)(\vec{\rho}\bullet\vec{\rho})$	$\frac{1}{2}\left[-2\left(\vec{H}\vec{A}_{242}\bullet\vec{\rho}^2\right)(\vec{\rho}\bullet\vec{\rho})\right]$	$\vec{A}_{242} = {}_{ALIGN}\vec{A}_{242} - 2\sum_{j=1}^{N}\left(\frac{\bar{y}_j}{y_j}\right) {}_{FF}\vec{A}_{151,j}$
$\left(\frac{\bar{y}_j}{y_j}\right)^2 {}_{FF}\vec{A}_{151,j}\vec{H}^2\bullet\vec{\rho}^3$	$\frac{1}{4}\left(-3\vec{A}_{333}\vec{H}^2\bullet\vec{\rho}^3\right)$	$\vec{A}_{333} = {}_{ALIGN}\vec{A}_{333} - \frac{4}{3}\sum_{j=1}^{N}\left(\frac{\bar{y}_j}{y_j}\right)^2 {}_{FF}\vec{A}_{151,j}$
$6\left(\frac{\bar{y}_j}{y_j}\right)^2\left({}_{FF}\vec{A}_{151,j}\bullet\vec{H}\right)\left(\vec{H}\bullet\vec{\rho}\right)(\vec{\rho}\bullet\vec{\rho})$ $3\left(\frac{\bar{y}_j}{y_j}\right)^2\left(\vec{H}\bullet\vec{H}\right)\left({}_{FF}\vec{A}_{151,j}\bullet\vec{\rho}\right)(\vec{\rho}\bullet\vec{\rho})$	$-2\left(\vec{H}\bullet\vec{A}_{331_M}\right)\left(\vec{H}\bullet\vec{\rho}\right)(\vec{\rho}\bullet\vec{\rho})$ $-\left(\vec{H}\bullet\vec{H}\right)\left(\vec{A}_{331_M}\bullet\vec{\rho}\right)(\vec{\rho}\bullet\vec{\rho})$	$\vec{A}_{331_M} = {}_{ALIGN}\vec{A}_{331_M} - 3\sum_{j=1}^{N}\left(\frac{\bar{y}_j}{y_j}\right)^2 {}_{FF}\vec{A}_{151,j}$
$2\left(\frac{\bar{y}_j}{y_j}\right)^3\left({}_{FF}\vec{A}_{151,j}\bullet\vec{H}\right)\left(\vec{H}^2\bullet\vec{\rho}^2\right)$ $2\left(\frac{\bar{y}_j}{y_j}\right)^3\left(\vec{H}\bullet\vec{H}\right)\left({}_{FF}\vec{A}_{151,j}\vec{H}\bullet\vec{\rho}^2\right)$	$\frac{1}{2}\left[-2\left(\vec{H}\bullet\vec{A}_{422}\right)\left(\vec{H}^2\bullet\vec{\rho}^2\right)\right]$ $\frac{1}{2}\left[-2\left(\vec{H}\bullet\vec{H}\right)\left(\vec{H}\vec{A}_{422}\bullet\vec{\rho}^2\right)\right]$	$\vec{A}_{422} = {}_{ALIGN}\vec{A}_{422} - 2\sum_{j=1}^{N}\left(\frac{\bar{y}_j}{y_j}\right)^3 {}_{FF}\vec{A}_{151,j}$
$6\left(\frac{\bar{y}_j}{y_j}\right)^3\left(\vec{H}\bullet\vec{H}\right)\left({}_{FF}\vec{A}_{151,j}\bullet\vec{H}\right)(\vec{\rho}\bullet\vec{\rho})$	$-4\left(\vec{H}\bullet\vec{H}\right)\left(\vec{A}_{420_M}\bullet\vec{H}\right)(\vec{\rho}\bullet\vec{\rho})$	$\vec{A}_{420_M} = {}_{ALIGN}\vec{A}_{420_M} - \frac{3}{2}\sum_{j=1}^{N}\left(\frac{\bar{y}_j}{y_j}\right)^3 {}_{FF}\vec{A}_{151,j}$

[a]From J. Opt. Soc. Am. A **26**, 1090-1100 (2009).
[b]From J. Opt. Soc. Am. A **27**, 1490-1504 (2010).
[c]From J. Opt. Soc. Am. A **28**, 821-836 (2011).

#217287 - $15.00 USD Received 18 Jul 2014; revised 12 Sep 2014; accepted 22 Sep 2014; published 20 Oct 2014

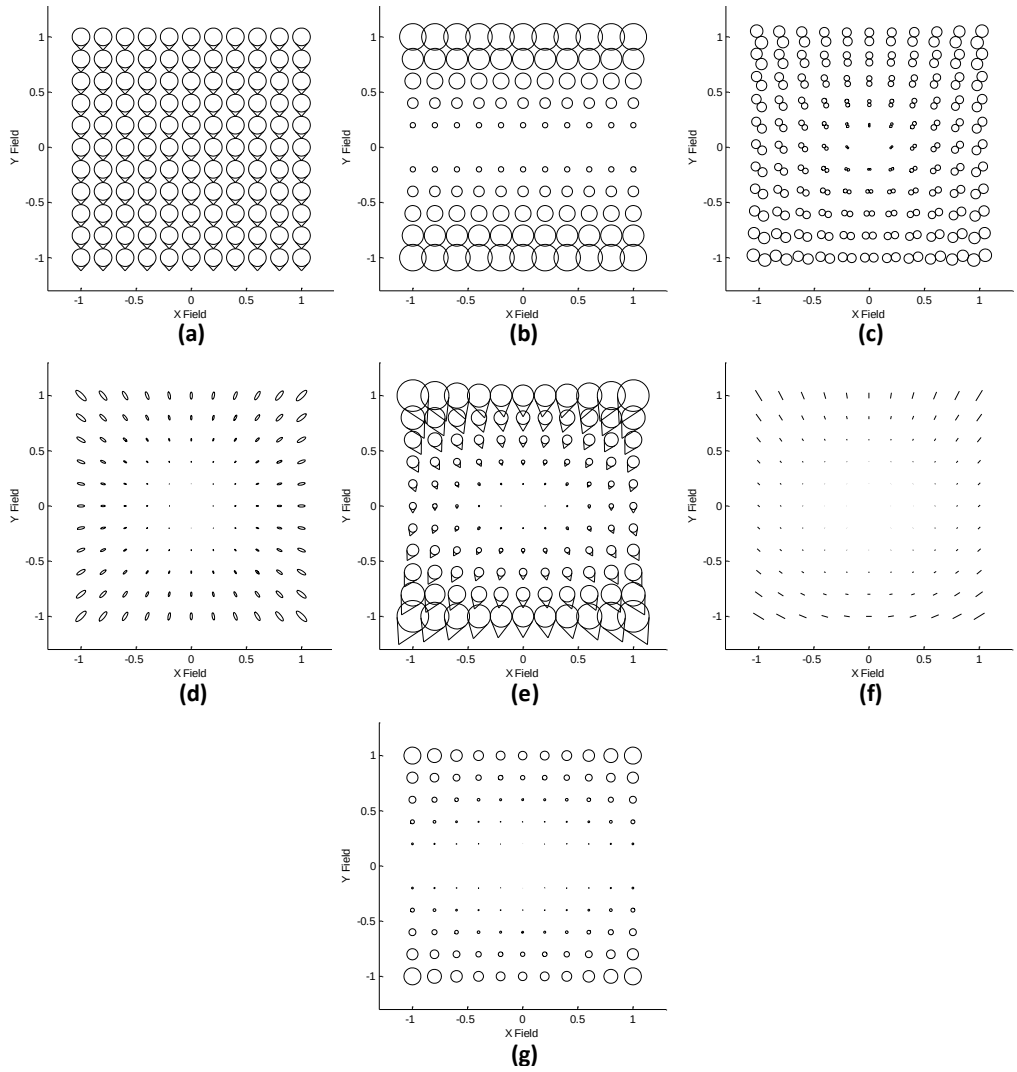

Fig. 8. The characteristic field dependence of (a) field constant, fifth order aperture coma, (b) field linear medial oblique spherical aberration, (c) field asymmetric, field linear oblique spherical aberration, (d) field quadratic trefoil, (e) hybrid field quadratic coma that is a combination of two field quadratic coma terms, (f) hybrid field cubic astigmatism that is a combination of two field cubic astigmatism terms, and (g) field cubic, medial field curvature that is generated by a Zernike fifth order aperture coma overlay on an optical surface away from the stop surface.

The magnitude and orientation plots of the aberration terms generated by a Zernike fifth order aperture coma overlay, summarized in Table 4, are depicted throughout the field in Figs. 8(a)–8(g). In Fig. 8(a), the field constant fifth order aperture coma contribution from a Zernike fifth order aperture coma overlay is displayed. The magnitude and orientation are the same everywhere throughout the field and are governed by the vector describing the overlay term, ${}_{FF}\vec{A}_{151}$. In Fig. 8(b), the medial oblique spherical aberration contribution from a Zernike fifth order aperture coma overlay away from the stop is displayed. The field behavior of this term resembles that of the medial field curvature term generated by a Zernike coma overlay. Figure 8(c) displays the oblique spherical aberration contribution where the field behavior resembles that of field asymmetric, field linear astigmatism. The elliptical coma contribution,

#217287 - $15.00 USD Received 18 Jul 2014; revised 12 Sep 2014; accepted 22 Sep 2014; published 20 Oct 2014

displayed in Fig. 8(d), is field quadratic and depending on the vector describing the overlay term, ${}_{FF}\vec{A}_{151}$, the aberration orientation may appear rotationally symmetric. In Fig. 8(e), the two field quadratic coma contributions are displayed together resulting in a hybrid field asymmetric aberration. Similarly, Fig. 8(f) displays together the two field cubic, fifth order astigmatism contributions, resulting in a hybrid aberration that is field asymmetric. Lastly, Fig. 8(g), displays a fifth order medial field curvature contribution that equates to a cubic shaped focal plane.

4. Higher order φ-polynomial surface overlays and their aberration fields

Currently, NAT only describes the aberration behavior up to sixth order in wavefront. For many optical systems, sixth order is sufficient; however, as the field and aperture continue to increase, higher order components (i.e. eighth order) may begin to contribute [10]. Also, the benefits of higher order φ-polynomial overlays (i.e. Fringe Zernikes greater than Z16) have been demonstrated in the design of a freeform Offner relay where tetrafoil was used as a variable to minimize astigmatism [22]. Using the procedure described in Section 3, the extension of NAT to freeform surfaces can be inferred to higher order components. As a relevant example, consider Zernike tetrafoil (Fringe polynomial terms Z_{17} and Z_{18}) that, in optical metrology terminology, is written as

$$\left(z_{17}\ z_{18}\right)\begin{pmatrix} Z_{17} \\ Z_{18} \end{pmatrix} = \left(z_{17}\ z_{18}\right)\begin{pmatrix} \rho^4\cos(4\phi) \\ \rho^4\sin(4\phi) \end{pmatrix}, \tag{54}$$

where z_{17} and z_{18} are the coefficient values for the tetrafoil term. The magnitude, ${}_{FF}\left|z_{17/18}\right|$, and orientation, ${}_{FF}\xi_{17/18}$, of the Zernike tetrafoil is then calculated from the coefficients as

$${}_{FF}\left|z_{17/18}\right| = \sqrt{z_{17}^2 + z_{18}^2}, \tag{55}$$

$${}_{FF}\xi_{17/18} = \frac{\pi}{2} - \frac{1}{4}\tan^{-1}\left(\frac{z_{18}}{z_{17}}\right). \tag{56}$$

The overlay term in Eq. (54) is linked to the vector multiplication environment of NAT with the following observation,

$$\textit{if } \vec{\rho} = \rho\begin{pmatrix} \sin(\phi) \\ \cos(\phi) \end{pmatrix}, \quad \textit{then } \vec{\rho}^4 = \rho^4\begin{pmatrix} \sin(4\phi) \\ \cos(4\phi) \end{pmatrix}, \tag{57}$$

where a right-handed coordinate system is employed with ϕ measured clockwise from the $\hat{y}-$axis. From the vector pupil dependence in Eq. (57), it is deduced that the tetrafoil deformation will induce field constant tetrafoil when located at the stop surface and is added to the total aberration field as

$$W_{Stop} = \frac{1}{8}\left({}_{FF}\vec{D}^4_{444} \bullet \vec{\rho}^4\right), \tag{58}$$

where ${}_{FF}\vec{D}^4_{444}$ is a two-dimensional vector that describes the magnitude and orientation of field constant tetrafoil, which is related to the overall Zernike tetrafoil by

$${}_{FF}\vec{D}^4_{444} \equiv 8(n'-n)\ {}_{FF}\left|z_{17/18}\right|\exp\left(i4\ {}_{FF}\xi_{17/18}\right). \tag{59}$$

#217287 - $15.00 USD Received 18 Jul 2014; revised 12 Sep 2014; accepted 22 Sep 2014; published 20 Oct 2014

Now replacing $\vec{\rho}$ with $\vec{\rho}'+\Delta\vec{h}$ in Eq. (59), expanding the pupil dependence, and simplifying leads to a specific set of additive terms for the wavefront expansion when a surface with a Zernike tetrafoil overlay is located away from the stop,

$$\begin{aligned} W_{Not\ Stop} &= \frac{1}{8}\left[{}_{FF}\vec{D}^{4}_{444} \bullet \left(\vec{\rho}'+\Delta\vec{h}\right)^{4} \right] \\ &= \frac{1}{8}\left[\begin{array}{l} {}_{FF}\vec{D}^{4}_{444} \bullet \vec{\rho}^{4} + 4\,{}_{FF}\vec{D}^{4}_{444}\Delta\vec{h}^{*} \bullet \vec{\rho}^{3} + 6\,{}_{FF}\vec{D}^{4}_{444}\Delta\vec{h}^{*2} \bullet \vec{\rho}^{2} \\ +4\,{}_{FF}\vec{D}^{4}_{444}\Delta\vec{h}^{*3} \bullet \vec{\rho} + {}_{FF}\vec{D}^{4}_{444} \bullet \Delta\vec{h}^{4} \end{array} \right], \end{aligned} \tag{60}$$

where the primes on the pupil coordinate have been dropped from the final expression and the vector identity in Eq. (11) is used to convert the pupil dependence into existing aberration types. In Eq. (60), four additional field dependent aberration terms are generated in addition to the anticipated field constant tetrafoil term. Table 5 displays the image degrading aberration terms generated by the Zernike tetrafoil overlay with $\Delta\vec{h}$ replaced in each term. Since these aberration components are not currently predicted by NAT, they cannot be linked to existing aberration components though their pupil dependences gives insight into their aberration behavior. In order of decreasing pupil dependence, the first term is field constant tetrafoil. The second term is an elliptical coma aberration based on the $\vec{\rho}^{3}$ dependence where the aberration is linear with the conjugate field dependence. The third term is an astigmatic aberration based on the $\vec{\rho}^{2}$ dependence where the aberration is quadratic with the conjugate field dependence.

Table 5. Image Degrading Aberration Terms That Are Generated by a Zernike Tetrafoil Overlay and How the Terms Link to Existing Concepts of NAT

Aberration Terms for a Zernike Tetrafoil Overlay	NAT Analog
$\frac{1}{8}\,{}_{FF}\vec{D}^{4}_{444,j} \bullet \vec{\rho}^{4}$	None
$\frac{1}{2}\left(\frac{\bar{y}_j}{y_j}\right){}_{FF}\vec{D}^{4}_{444,j}\vec{H}^{*} \bullet \vec{\rho}^{3}$	None
$\frac{3}{4}\left(\frac{\bar{y}_j}{y_j}\right)^{2}{}_{FF}\vec{D}^{4}_{444,j}\vec{H}^{*2} \bullet \vec{\rho}^{2}$	None

The magnitude and orientation plots of the aberration terms generated by a Zernike tetrafoil overlay, summarized in Table 5, are depicted throughout the field in Figs. 9(a)–9(c). In Fig. 9(a), the field constant tetrafoil contribution is displayed. The magnitude and orientation are the same everywhere throughout the field and are governed by the vector describing the overlay term, ${}_{FF}\vec{D}^{4}_{444}$. In Fig. 9(b), the elliptical coma contribution from a Zernike tetrafoil overlay away from the stop is displayed. The field behavior of this term resembles that of the astigmatic term generated by a Zernike elliptical coma overlay. Figure 9(c) displays the astigmatic contribution that is quadratic with the field conjugate vector so the field behavior takes on a unique orientation never seen before in the context of NAT.

#217287 - $15.00 USD Received 18 Jul 2014; revised 12 Sep 2014; accepted 22 Sep 2014; published 20 Oct 2014

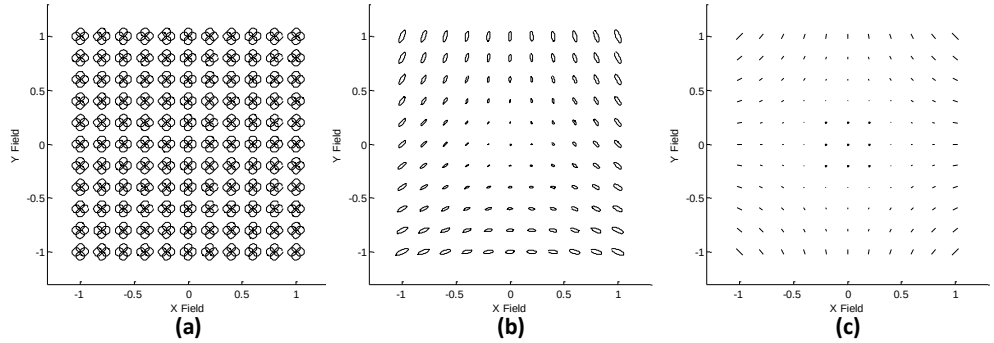

Fig. 9. The characteristic field dependence of (a) field constant tetrafoil, (b) field conjugate, field linear trefoil, and (c) field conjugate, field quadratic astigmatism which is generated by a Zernike tetrafoil overlay on an optical surface away from the stop surface.

5. Conclusion

We have presented how, for the first time, an important class of freeform optical surfaces, known as φ-polynomial (Zernike) surfaces, may be integrated with nodal aberration theory (NAT) to yield a complete theory of aberrations that includes freeform surfaces in nonsymmetric optical system design. Depending on the location of the freeform surface in the optical system, the freeform surface net aberration contribution may be field dependent and will contribute aberration field components that are of lower radial order than the φ-polynomial surface types applied to the surface. Significantly, we have found that the aberrations components induced by a freeform surface link directly to existing concepts of NAT. Consistent with NAT, there are no new aberration types, only more complex field dependences. These aberration components were first developed in the context of NAT as misalignment induced components of the fourth and sixth order wavefront aberrations but have not been isolated until now. In nonsymmetric optical systems with large tilts and decenters, these fourth and sixth order modifications to the field dependence of the wave aberrations are often the dominant performance limiting aberrations and reveal why freeform surfaces are useful in improving the performance of the nonsymmetric optical system.

We have presented each of the aberration fields that result in image degradation through Fringe Zernike term 17/18 (tetrafoil) and demonstrated the mapping to terms originally derived in NAT. While it was not directly demonstrated, the 1:1 mapping of the freeform surface field aberrations to existing NAT terms means that the specific nodal geometries that are established by NAT, which are wave aberration type unique, will be characteristic features when full field analysis is conducted during freeform optical system design. With this foundation in place, optical design strategies are being applied to fully nonsymmetric imaging optical systems with freeform surfaces based on nodal control point optimization.

Acknowledgments

We thank the Frank J. Horton Research Fellowship of the Laboratory for Laser Energetics, the II-VI Foundation, the National Science Foundation (EECS-1002179), and the NYSTAR Foundation (C050070) for supporting this research. We also thank the NSF I/UCRC Center for Freeform Optics (CeFO) academic and industry members for stimulating discussion about this research.

#217287 - $15.00 USD Received 18 Jul 2014; revised 12 Sep 2014; accepted 22 Sep 2014; published 20 Oct 2014